PROCEEDINGS OF SCIENCE

The SPI High Energy Sky

Jean-Pierre Roques[1]
CESR/CNRS
9,av. Du Colonel Roche 31028 Toulouse, France
E-mail: Jean-Pierre.Roques@cesr.fr

We present here a summary of 7 years of observation at high energy with the SPI onboard the Integral spacecraft. SPI is a spectrometer working in the 20 keV - 8 MeV energy range providing an unprecedented energy resolution over a large period of time.

We will review the status of this instrument and we will demonstrate its quality and stability through key parameters: the energy resolution, gain calibration and the spectral response.

SPI contributes to unveil the high energy sky thanks to its wide energy range, its wide field of view and a compromise between a moderate angular resolution (2.6°) and sensitivity to diffuse emissions.

We discuss the current status of the annihilation radiation of the Galactic disk and show that it is well described by a bulge and a symmetric disk components.

The spectroscopic properties of the instrument are well illustrated by the measurement of the energy shift of the ^{26}Al gamma-ray line along the Galactic plane.

Thanks to its "hybrid" imaging characteristics, SPI is able to disentangle the diffuse emission of the Galactic ridge and the emission of point sources giving a coherent global picture of the high energy emission of our Galaxy.

Concerning the emission of the compact objects, SPI confirms and demonstrates that a high energy tail can be present in their spectra, above the standard thermal Comptonisation component. This high energy emission and its variability are under study and will provide new tests to understand the mechanisms at work in these objects.

The Extreme sky: Sampling the Universe above 10 keV - extremesky2009
Otranto (Lecce) Italy
October 13-17, 2009

[1] Speaker

PoS(extremesky2009)005

1.SPI Status

The SPI camera is composed of 19 Germanium detectors working at 80 K. During these 7 years of operation we experienced the failure of 3 detector chains. While their cause is largely unknown, these failures happen on detectors without precursor sign and we tried to optimize all the operations in order to limit the potential risks. We should stress that, after 7 years in orbit, 85% of the detector plane is working with nominal performance.

This camera is surrounded by a massive active BGO shield exhibiting good and stable performance despite the failure of two FEEs. Thanks to the redundancy concept of the BGO shield these failures didn't impact SPI background rejection.

Due to the decrease of the solar activity reinforced by the extended solar minimum, the background of the instrument has roughly doubled since the launch. Figure 1 shows the evolution of the solar cycle and the evolution of the ACS counting rate since 2005 together with the SPI telemetry usage. We can see that despite the high background increase, SPI telemetry has been kept below 105 pkt/cycle (5.75 kbytes/s). This has been possible through intensive and regular on-board software improvements implementing various on-board compression algorithms.

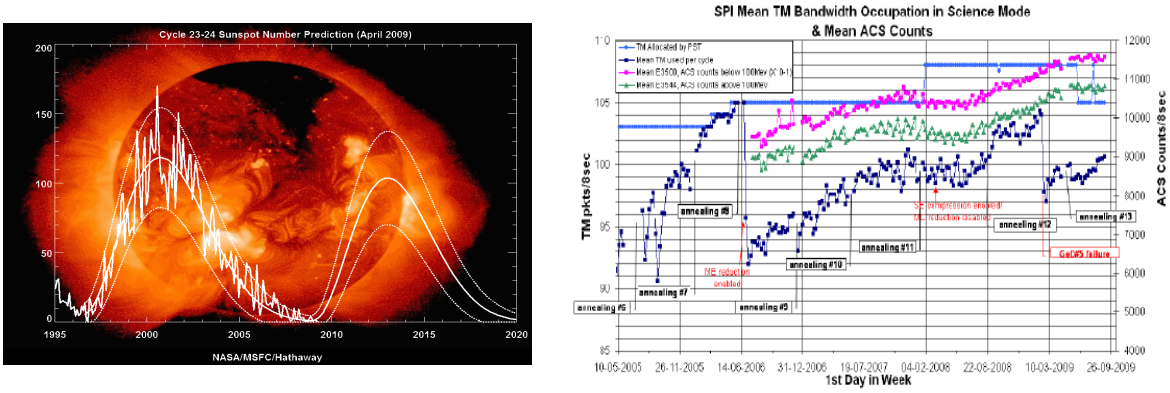

Figure 1: Left: solar sunspot number and prediction. Right: SPI counting rate evolution (green and pink) together with the telemetry usage (blue) since may 2005.

During these seven years, we have been able to keep the outstanding energy resolution of the SPI camera thanks to a design allowing regular annealing of the detector plane. These annealing operations, performed with six month intervals, consist in heating the detector plane up to 105° C during 200 hours. This process allows restoring the original spectroscopic properties of detectors damaged by irradiation by cosmic rays.

Figure 2 shows the evolution of the 1764.3 keV background line over the mission. It can be seen that the energy resolution of the instrument has been kept under control since the launch.

PoS(extremesky2009)005

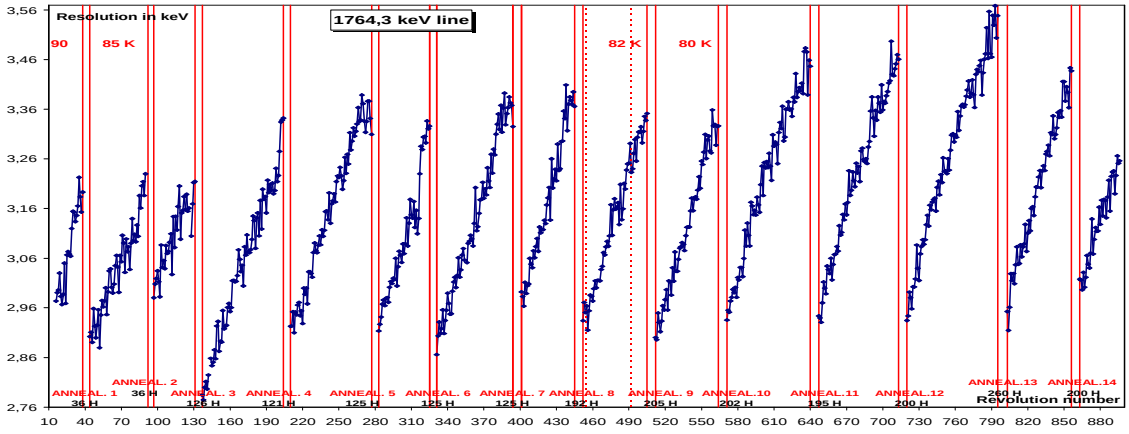

Figure 2: Energy resolution history of the 1764 keV line during 7 years.

2. SPI ENERGY CALIBRATION

The energy calibration is a crucial point for such a telescope since its stability has a direct impact on the energy resolution, on the matching between detectors and between observations versus time.

Currently, the energy calibration is performed for each detector on a per revolution basis using background gamma-ray lines. In the low energy range, i.e. between 20 keV and 2 MeV, 6 lines are fitted while 2 lines are used in the 2-8 MeV range. In the low energy range the channel (C)

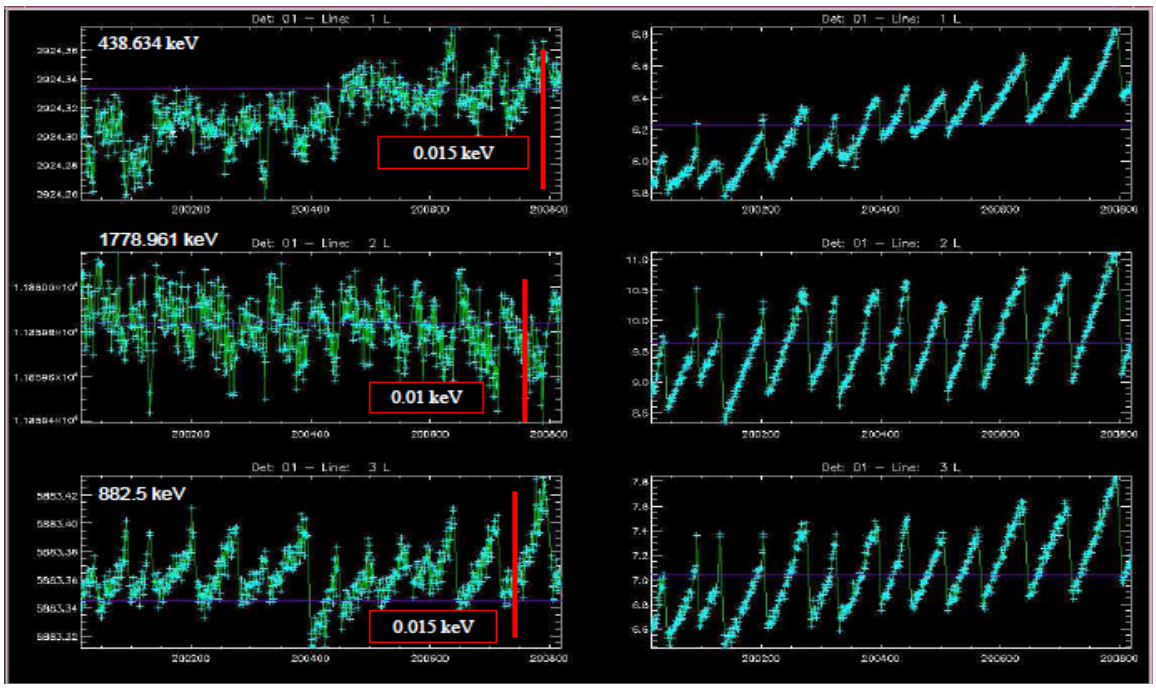

Figure 3: Reconstructed line position (left panels) – Energy resolution (right panels)

PoS(extremesky2009)005

to energy (E) relation has the form: $E = a\ Log(C) + b + c\ C + d\ C^2 + e\ C^3$ while a simple linear function is used for the high energy range.

In order to check the energy calibration, we build a spectrum for each revolution using all calibrated photons of all detectors. Then we study the position and energy resolution of several background lines. Figure 3 displays the results for 3 lines: we see that the line positions are stable within 0.015 keV (left panels) while the right panels show the energy resolution degradation due to the irradiation and its recovery after each annealing.

2. Observation of the Crab

While regular observations are performed about each 6 months on the Crab Nebula in order to check all instruments performance, a dedicated campaign has been obtained in 2008 in the standard 5X5 pattern. This long exposure allowed us to investigate some instrumental issues linked to systematic effect (seen above ~ 700 keV and identified with saturating events) or stability of the gain correction and instrument efficiency at high energy.

Three mean Crab spectra obtained through the mission are presented in figure 4 together with best fit parameters of these three periods (Table 1). The perfect agreement between all values demonstrates clearly that we get reliable data up to a few MeV in the standard 5X5 pattern [1].

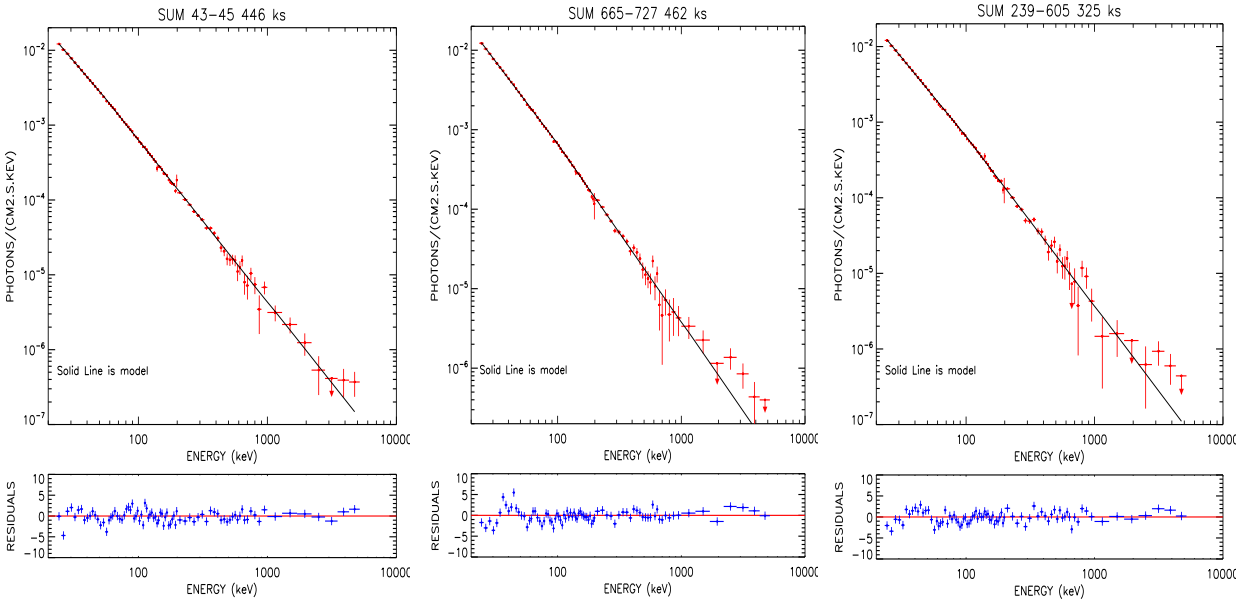

Figure 4: Crab spectra for three periods 2003 (left); 2004-2007 (middle); 2008 (right).

A simultaneous fit of these three spectra with a broken power law model (and 0% systematic) gives the following parameters: index1=2.04; index2= 2.18; Break energy=62 keV. It is worth to mention that the spectrum seems to show a gradual steepening of the slope instead

PoS(extremesky2009)005

of a localised break. Our Crab spectrum is indeed better fitted with $\mathbf{F(E) = N \cdot E^{a+b.log(E/E0)}}$. In this case we found with E0 fixed to 20 keV: a=1.79, b=0.134 and N= 3.97 ph/cm²/s/keV.

We want to point out that our Crab spectrum only relies on ground calibrations and SPI response modelling. Hence this spectrum can be considered as absolute.

In addition, the analysis of the Crab pulsar demonstrated the timing performance of the instrument and showed the energy dependence of the time lag between radio and X-rays [13].

Rev #	Index 1	Ebreak (fixed)	Index 2	Norme @ 100 keV
2003	2.07	100 keV	2.24	6.6 10^{-4} ph/cm2 s.keV
2004-2007	2.07	100 keV	2.25	6.55 10^{-4} ph/cm2 s.keV
2008	2.065	100 keV	2.25	6.7 10^{-4} ph/cm2 s.keV

Table 1: Broken power law spectral fit parameters for the 3 periods.

3.All sky Survey

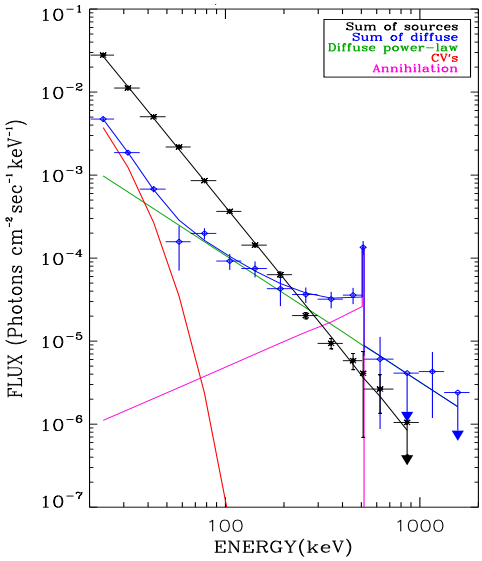

Figure 5: Galactic Ridge spectral components.

A hard work (over years!) has been done on data analysis methods by the instrument team:

- An automatic analysis tool, SPImodfit, developed at MPE, provides spectra by revolution for 100 sources. The main results are presented in [2]

- CESR tools allow to treat all data simultaneously; this provides catalogs, mean spectra and light curves of more than 200 sources together with diffuse emission analysis, see [3], [4], [5].

As main results of this later work, the global Galaxy spectrum decomposed in its various components is displayed in fig 5. This work is based on the use of 6 years of data and on new algorithms to handle huge data sets and sky variability with a segmentation method. The main goal is to determine the Galactic diffuse emission spectrum, once the individual source and annihilation process contributions have been removed. SPI data have been modeled with the Galprop model [6] and provide improved constrains on the diffuse emission production [5].

PoS(extremesky2009)005

4.The annihilation radiation: still a mystery

The morphology of the 511 keV emission is still controversial. While Weidenspointner et al. [7] claimed for an asymmetric disk emission, Bouchet et al. [4] showed an emission symmetric with respect to the Galactic Center.

An update including new data is given by Bouchet et al. [5]. Here too, data have to be deconvolved simultaneously to obtain the spatial distribution of this peculiar emission. 6 yr of data has been analyzed through 2 different approaches. A model independent map has first been produced (figure 6, left) by determining the flux coming from individual sky pixels (5x5 degrees). In another side, its spatial geometry has been tested by model fitting against various maps observed at other wavelengths and analytical shapes. Finally, we find that the annihilation emission occurs mostly in the bulge which can be described at the first order by 2 Gaussians while an extended component (Galactic disk) appears thanks to the data accumulation. For this latter, its global flux is very sensitive to the assumed model but its distribution is compatible with a symmetric distribution (figure 6 right).

This study is very important to understand the origin of the Galactic positron population and numerous works have been triggered by these observations. Concerning the potential sources of positrons, Sgr A, pulsars, binaries and dark matter have been suggested by different authors. Positron propagation has also been studied as well as annihilation physics and sites.

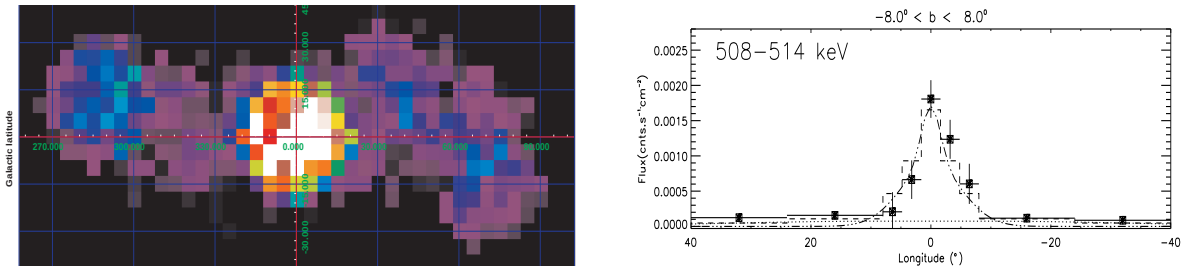

Figure 6: left, map of the 511 keV emission. Right: Galactic longitude profile at 511 keV**.**

5. Observation of ^{26}Al production sites. Line shift measurement

Thanks to the very good stability of the instrument, the energy calibration can be very precise. Hence the centroid and width of astrophysical gamma-ray lines can be reliably derived. The results related to the Galactic emission of the gamma-ray line at 1.8 MeV which traces the ^{26}Al nuclei production sites are a good illustration. A global view of the Galactic plane is displayed in figure 7 with the different emission regions while the figure in the top right corner, through the relation between the line centroid shift and the longitude site, illustrates the effect of the rotation of the Galaxy (Doppler shift), providing the definitive proof that the observed emission is produced in the disk [8].

PoS(extremesky2009)005

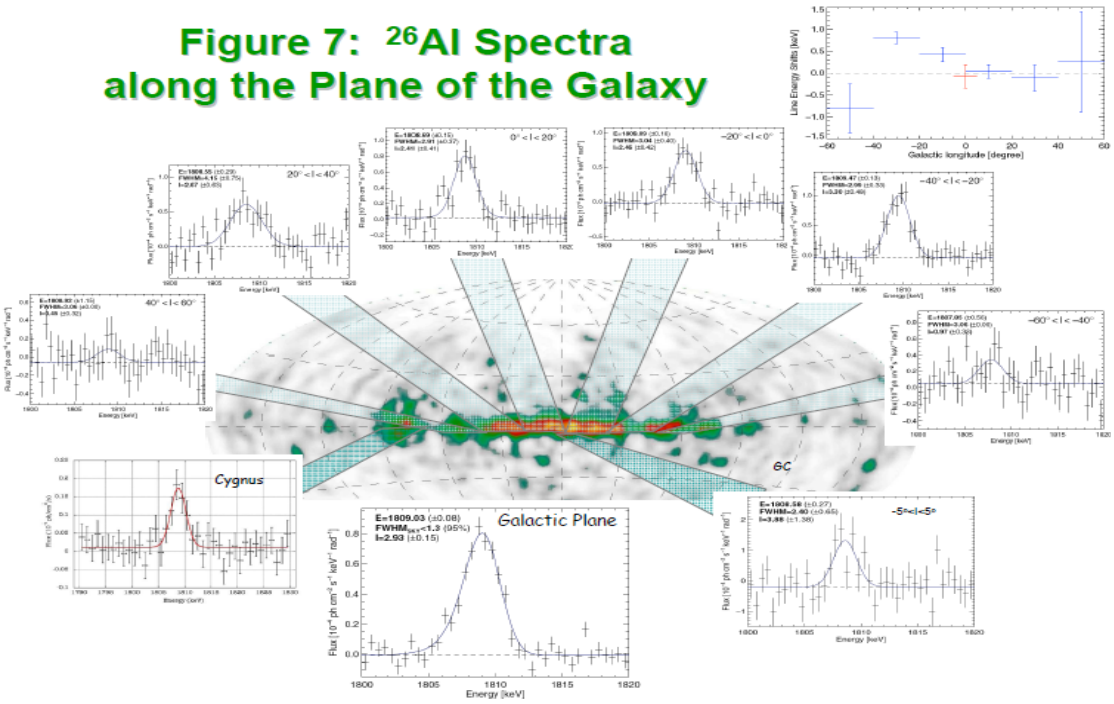

6.High Energy Tail in Compact Objects

Thanks to its extended energy range and good sensitivity at high energy, SPI is able to observe compact objects up to the MeV region. Moreover, with the Crab observations, we demonstrated that SPI produces very stable and reliable results from 20 keV to a few MeV thus allowing detailed studies of the high energy component in the spectra of individual sources.
When present, such a hard spectral component is characterised by an excess of flux relatively to the “classical” comptonisation law above ~100 keV and extending up to a few hundreds of keV, see [10], [11], [12].

- 1E1740.7: Figure 8 left shows the spectrum of the source as observed by SPI and IBIS in the hard state. The spectrum is similar to Cygnus X-1 and can be represented by a 2 components spectral model [9]

-Cygnus X-1: The “mean” spectrum of Cygnus X-1 as observed by SPI is presented in figure 8 middle panel. The spectrum extends up to 700 keV and can be represented by a 2 components comptonisation model whose temperatures are 43 kev and 100 keV (fixed) plus a reflection component.

The presence of such a hard energy tail imposes a more complex description of the data than the standard comptonisation law. The added component can be interpreted as a second componisation region, a pair plasma component or a non thermal emission that could originate from a jet.

PoS(extremesky2009)005

This high energy extension is observed in compact objects containing a black hole candidate for the vast majority. Nevertheless we point out the case of the neutron start system GS1826-24 which exhibits a spectrum up to 500 keV, figure8 right, in this case the hard component can be reprented by a power law of index 2 above a thermal comptonisation with a temperature of 18 keV.

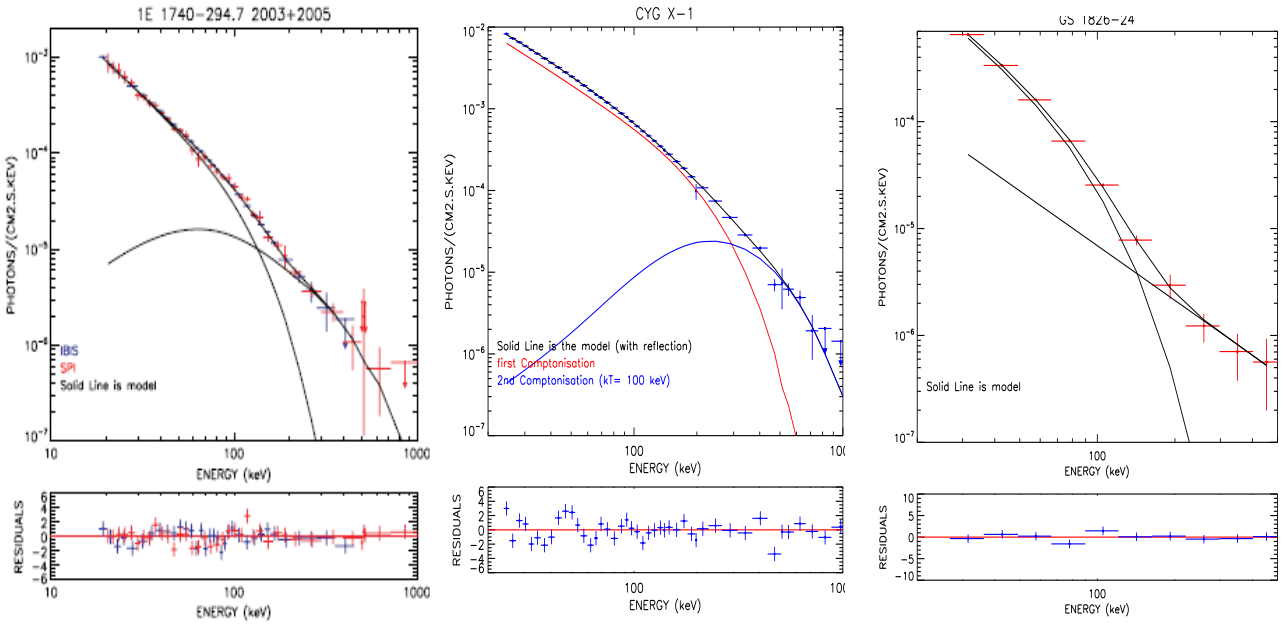

Figure 8: The high energy tail of three compact objects.

7.Conclusion

- During these 7 years of operation in space SPI continues to exhibit nominal performance and in particular its energy resolution is kept under control and the energy conversion is stable and precise.
- Instrument stability and control of systematics up to a few MeV has been validated through Crab data analysis.
- **SPI is a unique instrument providing reliable spectra up to a few MeV allowing detailed spectral analysis**
- An all sky survey has been performed using 6 years of data providing a global picture of the Galaxy in hard X-ray
- 511 keV emission morphology is well described by a bulge component (composed by two axisymmetric Gaussians) and a symmetric disk component. Its origin is still unknown!
- Study of compact object spectra and hard tail components gives new insights of the physics at work stimulating new numerical modelling effort.

PoS(extremesky2009)005

References

[1] Jourdain, E.; Roques, J. P, 2009 ApJ, 704,17-24.

[2] Petry, D. ; Beckmann, V. ; Halloin, H. et al., 2009, A&A, 507,549.

[3] Bouchet, L. ; Jourdain ; E., Roques, J.-P. ; et al., 2008,ApJ, 679,1315.

[4] Bouchet, L.; Roques, J. P. ; Mandrou, et al. ; 2005, ApJ, 635, 1103.

[5] Bouchet, L ; Strong, A. ; Jourdain, E. ; et al., This conference.

[6] Strong, A ;, Moskalenko, I. ; Reimer ; 2004, ApJ, 613, 956.

[7] Weidenspointner , G., Skinner, G.; Jean, P.; 2008, Nature, 451, 159.

[8] W ang, W.; Lang, M. G.; Diehl, R.; et al., 2009, A&A, 496,713-724.

[9] Bouchet, L.; del Santo, M.; Jourdain, E.; Roques, J. P.; et al., 2009, ApJ 693, 1871-1876.

[10] Jourdain, E. Roques, J-P. ; Bouchet, L. ; 2007, PThPS, 169, 221.

[11] Droulans, R. ; Jourdain, E. ; 2009, A&A, 494, 229.

[12] Joinet, A. ; Jourdain, e.; Malzac, E.; 2007, 657, 400.

[13] Molkov, S.; Jourdain, E.; Roques, J. P. ,2010, ApJ,708,403.

